p190RhoGAP is the convergence point of adhesion signals from $\alpha_5\beta_1$ integrin and syndecan-4

Mark D. Bass,[1] Mark R. Morgan,[1] Kirsty A. Roach,[1] Jeffrey Settleman,[2] Andrew B. Goryachev,[3] and Martin J. Humphries[1]

[1]Wellcome Trust Centre for Cell-Matrix Research, Faculty of Life Sciences, University of Manchester, Manchester M13 9PT, England, UK
[2]Massachusetts General Hospital Cancer Center, Harvard Medical School, Charlestown, MA 02129
[3]Centre for Systems Biology, School of Biological Sciences, University of Edinburgh, Edinburgh EH9 3JR, Scotland, UK

The fibronectin receptors $\alpha_5\beta_1$ integrin and syndecan-4 cocluster in focal adhesions and coordinate cell migration by making individual contributions to the suppression of RhoA activity during matrix engagement. p190Rho–guanosine triphosphatase–activating protein (GAP) is known to inhibit RhoA during the early stages of cell spreading in an Src-dependent manner. This paper dissects the mechanisms of p190RhoGAP regulation and distinguishes the contributions of $\alpha_5\beta_1$ integrin and syndecan-4. Matrix-induced tyrosine phosphorylation of p190RhoGAP is stimulated solely by engagement of $\alpha_5\beta_1$ integrin and is independent of syndecan-4. Parallel engagement of syndecan-4 causes redistribution of the tyrosine-phosphorylated pool of p190RhoGAP between membrane and cytosolic fractions by a mechanism that requires direct activation of protein kinase C α by syndecan-4. Activation of both pathways is necessary for the efficient regulation of RhoA and, as a consequence, focal adhesion formation. Accordingly, we identify p190RhoGAP as the convergence point for adhesive signals mediated by $\alpha_5\beta_1$ integrin and syndecan-4. This molecular mechanism explains the cooperation between extracellular matrix receptors during cell adhesion.

Introduction

Membrane protrusion that is initiated at the leading edge of a spreading or migrating cell requires transient suppression of the contractile signals that lie downstream of the small GTPase RhoA. Engagement of adhesion receptors by the ECM provides a means of localizing this suppression (Burridge and Wennerberg, 2004; Raftopoulou and Hall, 2004). The two major families of ECM receptor use different modes of ligand binding: integrins bind directly to peptide sites within the ECM (Arnaout et al., 2005), whereas syndecans interact with heparin-binding motifs of ECM molecules through covalently linked glycosaminoglycan chains (Bernfield et al., 1999). The two families of adhesion receptors transduce synergistic signals to promote adhesion contact formation, and there are many examples of biological processes that are regulated by cooperative signaling by different integrin–syndecan pairs (Morgan et al., 2007). The prototypic fibronectin receptors, $\alpha_5\beta_1$ integrin and syndecan-4, colocalize in focal complexes at the leading edge of cells spreading on fibronectin (Woods et al., 2000), and several groups have demonstrated that simultaneous engagement of both receptors is necessary for the formation of vinculin-containing focal adhesions (Woods et al., 1986; Bloom et al., 1999; Bass et al., 2007a). Other groups have argued that integrin engagement is sufficient for focal adhesion formation (Wang et al., 2005), and the disagreement is partly due to the difficulty of eliminating syndecan ligands, which include growth factors and chemokines as well as ECM, from an experimental system. However, a greater contribution to this controversy arises from the robustness of the eukaryotic cell, which appears capable of surviving and adhering even under suboptimal conditions. It is becoming clear that rather than forming an integral part of the adhesive machinery, syndecans fine-tune signals downstream of receptors such as integrins and enable cells to respond rapidly and precisely to extracellular stimuli. The refined role of syndecan-4 is most apparent in vivo, as disruption of the syndecan-4 gene is not lethal but does compromise wound healing. Expression of both $\alpha_5\beta_1$ integrin and syndecan-4 is up-regulated in fibroblasts and keratinocytes surrounding dermal wounds (Cavani et al., 1993; Gallo et al., 1996), whereas disruption of syndecan-4 expression results in a delay in wound closure that is caused by a reduction in cell migration (Echtermeyer et al., 2001).

Correspondence to Martin J. Humphries: martin.humphries@manchester.ac.uk

Abbreviations used in this paper: BIM-1, bisindolylmaleimide 1; GAG, glycosaminoglycan; GAP, GTPase-activating protein; GEF, guanine nucleotide exchange factor; MEF, mouse embryonic fibroblast; p190-A, p190RhoGAP-A; TrX, Triton X-100.

The online version of this paper contains supplemental material.

© 2008 Bass et al.
The Rockefeller University Press $30.00
J. Cell Biol. Vol. 181 No. 6 1013–1026
www.jcb.org/cgi/doi/10.1083/jcb.200711129

THE JOURNAL OF CELL BIOLOGY

Downloaded from http://rupress.org/jcb/article-pdf/181/6/1013/1551983/jcb_200711129.pdf by guest on 08 February 2026

The specific involvement of syndecans in biological functions that are characteristic of higher vertebrates, such as wound healing, is supported by phylogenetic studies describing the evolution of duplicate syndecans that are highly conserved in vertebrates but absent from invertebrates (Chakravarti and Adams, 2006).

$\alpha_5\beta_1$ integrin and syndecan-4 activate Rac1 and inhibit RhoA to regulate membrane protrusion (Bass et al., 2007b). Unlike Rac1, where $\alpha_5\beta_1$ integrin and syndecan-4 regulate localization and GTP-loading, respectively (Del Pozo et al., 2004; Bass et al., 2007b), the GTP loading of RhoA is directly influenced by both receptors (Ren et al., 1999; Arthur et al., 2000; Dovas et al., 2006; Bass et al., 2007b) and could represent redundancy in activation of the RhoA signaling pathway. In the absence of evidence for direct receptor crosstalk, identification of the convergence point of integrin and syndecan signals has become a priority.

The ability of RhoA to associate with downstream effectors is held in balance by the opposing activities of guanine nucleotide exchange factors (GEFs) that stabilize the nucleotide-free form of RhoA and therefore encourage GTP loading, and GTPase-activating proteins (GAPs) that catalyze the low-level intrinsic GTPase activity of RhoA (Burridge and Wennerberg, 2004; Raftopoulou and Hall, 2004). ECM-dependent suppression of RhoA activity has been largely attributed to the action of p190RhoGAP-A (p190-A). Thus, a dominant-negative mutant of p190-A prevents the reduction in RhoA activity during adhesion to fibronectin and culminates in a delay in cell spreading and compromised migration toward fibronectin (Arthur and Burridge, 2001). In response to fibronectin binding, p190-A is tyrosine phosphorylated by a cascade involving the kinases Src (Arthur et al., 2000) and Arg (Bradley et al., 2006). Tyrosine phosphorylation of p190-A enables association with the SH2 domains of p120RasGAP that is necessary for the suppression of RhoA during cell spreading on fibronectin (Bradley et al., 2006). However, the connection from adhesion receptor to RhoA remains incomplete, as only a subset of integrins, which excludes β_1 integrins, activate Src by direct association (Arias-Salgado et al., 2005), and there is no evidence of a direct association between integrin and Arg. The only direct link from adhesion receptor to cytoplasmic kinase involves the activation of PKCα by direct association with the cytoplasmic domain of syndecan-4 (Koo et al., 2006). Interestingly, the activation of PKCα by stimulation with phorbol ester causes the redistribution of p190-A to membrane ruffles (Brouns et al., 2000) and may form a second regulatory mechanism. The challenge now is to establish the direct connection between an ECM receptor and p190-A that will explain adhesion-dependent RhoA regulation.

In the present study, we define a novel connection from syndecan-4 to p190-A, via PKCα, that results in redistribution of the GAP and, ultimately, inhibition of RhoA. Not only does this discovery fill in the missing link between adhesion receptor and RhoA regulation, it also distinguishes the contributions of syndecan-4 and $\alpha_5\beta_1$ integrin, which regulate p190-A through PKCα and tyrosine phosphorylation, respectively. These experiments identify p190-A as the convergence point for signals from coupled ECM receptors that is responsible for precisely localized RhoA regulation.

Results

Syndecan-4 regulates membrane association of p190-A

Fibroblasts plated onto a recombinant 50-kD fragment of fibronectin (50K), which encompasses the binding sites for $\alpha_5\beta_1$ integrin (Danen et al., 1995) but lacks a syndecan-4–binding motif, spread but fail to form vinculin-containing focal adhesions (Woods et al., 1986; Bloom et al., 1999; Bass et al., 2007a) because of a failure to regulate Rac1 (Bass et al., 2007b), RhoA (Dovas et al., 2006), and FAK (Wilcox-Adelman et al., 2002). The prespread fibroblasts respond rapidly to stimulation with a soluble syndecan-binding fragment of fibronectin, which comprises type III repeats 12–15 (H/0; Sharma et al., 1999), by regulating GTPases and forming focal complexes within 10 min of stimulation (Bass et al., 2007b). To delineate the relationship between these signals, engagement of integrin and syndecan-4 were separated temporally by treating fibroblasts with cycloheximide in order to prevent synthesis of syndecan-4 ligands and spreading the fibroblasts on 50K for 2 h before stimulating with H/0 over a time course. Potential changes in the levels of Triton X-100 (TrX)-soluble, tyrosine-phosphorylated proteins upon H/0 stimulation were examined. An immediate reduction in a 190-kD band, which is larger than the FAK and Cas bands that make up the majority of cellular tyrosine-phosphorylated protein, was observed in the 0.5% (wt/vol) TrX-soluble protein (Fig. 1 A) and could be explained by either dephosphorylation or redistribution of a protein between soluble and insoluble fractions. Lysates prepared in 1% (wt/vol) TrX, 0.5% (wt/vol) deoxycholate, and 0.1% (wt/vol) SDS did not show the same change (Fig. 1 B), which indicates that change in the abundance of the 190-kD band was caused by redistribution rather than a change in phosphorylation status. Having previously described the syndecan-4–dependent regulation of RhoA over this period (Bass et al., 2007b), we hypothesized that the change might represent redistribution of p190-A, which is known to mediate the suppression of RhoA activity during the initial phase of cell spreading on fibronectin (Ren et al., 1999; Arthur et al., 2000). Redistribution of p190-A in response to H/0 stimulation was analyzed by rupturing spread cells using 0.5% (wt/vol) TrX and clarifying lysates by centrifugation. Quantitative Western analysis using fluorophore-conjugated antibodies that enable direct measurement of relative protein levels revealed significant ($P = 0.0036$) redistribution of p190-A into the TrX-soluble fraction at 30 min, which diminished after extended stimulation of syndecan-4 (Fig. 1 C). Preparation of lysates in 1% (wt/vol) TrX, 0.5% (wt/vol) deoxycholate, and 0.1% (wt/vol) SDS confirmed that the total cellular level of p190-A did not change over the course of the experiment, and that observed changes were caused by redistribution rather than protein expression (see Fig. 6 A). As a control, cells were stimulated with a mutant of H/0 in which the heparin-binding motifs were mutated (H/0-glycosaminoglycan [GAG]), and no effect was observed on the levels of soluble p190-A (Fig. 1 D).

Downloaded from http://rupress.org/jcb/article-pdf/181/6/1013/1551983/jcb_200711129.pdf by guest on 08 February 2026

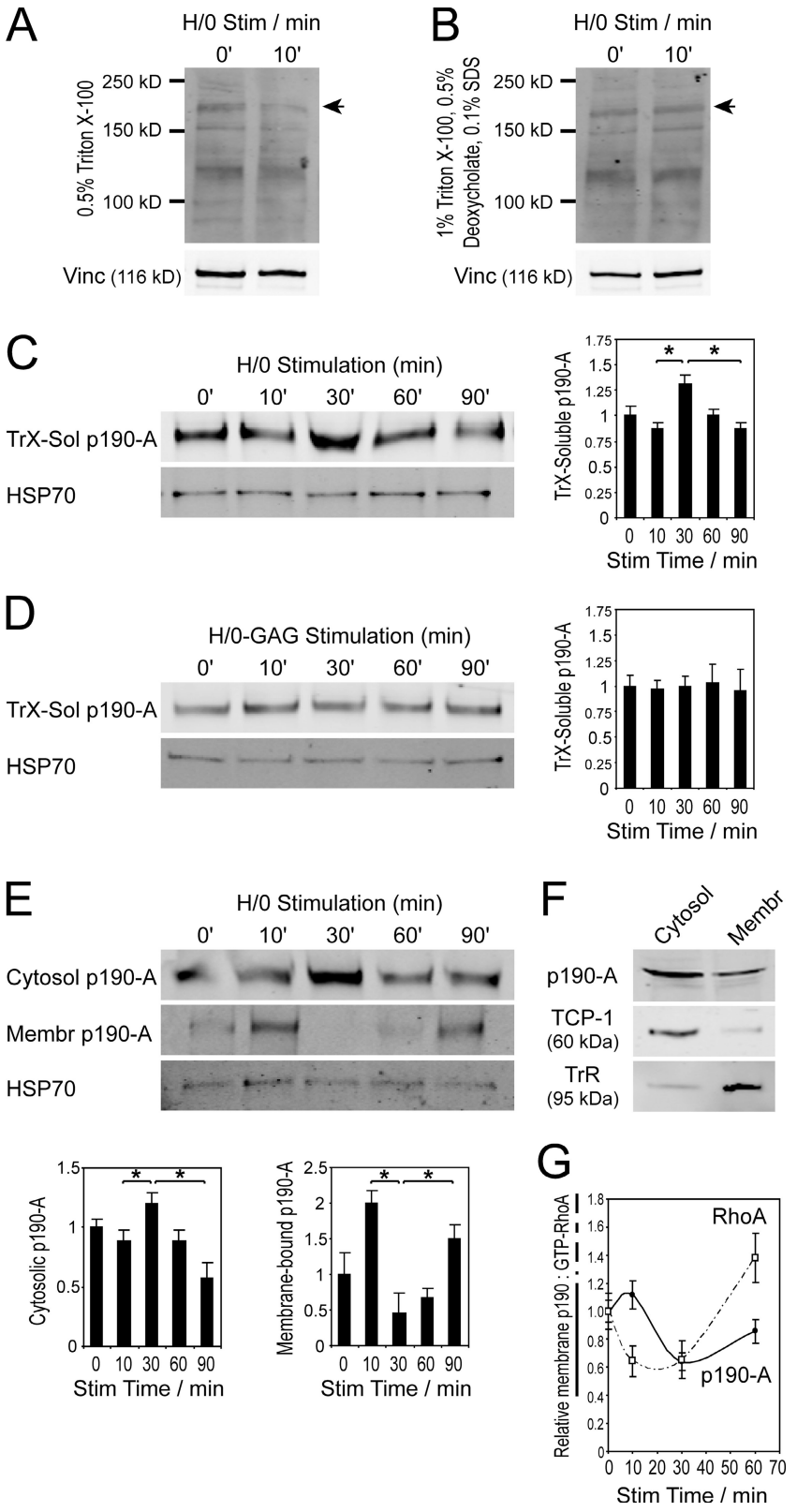

Figure 1. **Engagement of syndecan-4 regulates membrane association of p190-A.** Fibroblasts prespread on a recombinant integrin ligand (50K) were stimulated with heparin-binding fragments of fibronectin (H/0) before preparing lysates and measuring redistribution of proteins between soluble and membrane-bound fractions or RhoA activity by Western blotting. (A and B) Soluble, tyrosine-phosphorylated protein in lysates prepared in 0.5% (wt/vol) TrX or 1% (wt/vol) TrX, 0.5% (wt/vol) deoxycholate, and 0.1% (wt/vol) SDS. Arrowheads indicate a 190-kD band that varied in abundance between conditions. (C and D) TrX-soluble p190-A in lysates after stimulation with H/0 or a heparin-binding mutant (H/0-GAG). (E) Cytosolic and membrane-bound p190-A in sonication lysates. (F) Relative distribution of p190-A and cytosolic and membrane-bound markers, tailless complex polypeptide 1α and transferrin receptor, between membrane and cytosolic fractions of sonication lysates prepared from equal numbers of cells spread on 50K and stimulated with H/0 for 10 min. (G) Correlation between RhoA activity (dashed line) and membrane-associated p190-A (solid line). Equal loading between time points was confirmed by blotting for vinculin or HSP70. Error bars represent standard error. *, significant change ($P < 0.05$) from experiments repeated on at least four separate occasions.

The use of 0.5% TrX in lysate preparation raised the possibility that cell membranes were being partially solubilized. To test whether the changes were a true representation of redistribution between cytosolic and membrane-bound fractions, cells were lysed mechanically. Fibroblasts scraped off 50K-coated dishes in PBS were lysed by sonication, and nuclei were removed by low-speed centrifugation before using high-speed centrifugation to separate lysates into microsomal and soluble fractions, which are characterized by the presence of transferrin receptor and the cytosolic chaperone TCP-1α,

Downloaded from http://rupress.org/jcb/article-pdf/181/6/1013/1551983/jcb_200711129.pdf by guest on 08 February 2026

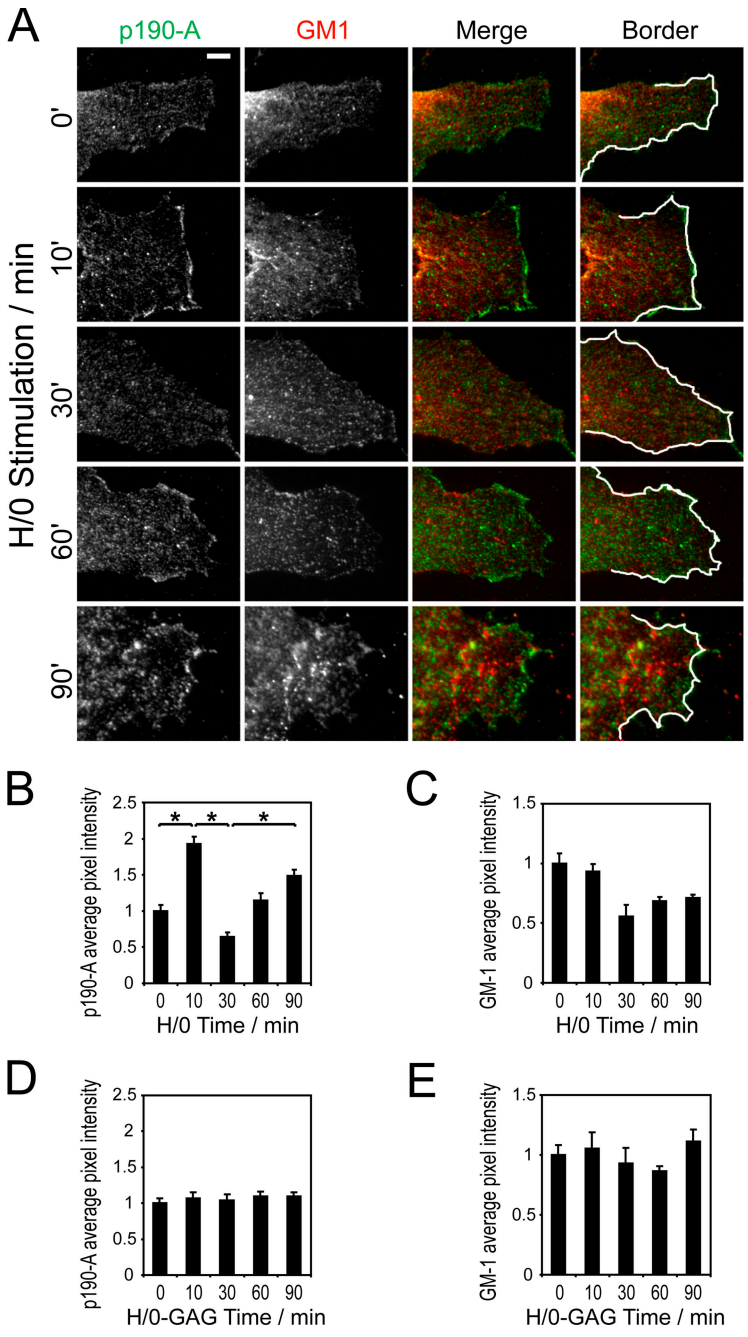

Figure 2. **p190-A is recruited to lamellae in response to engagement of syndecan-4.** Fibroblasts prespread on a recombinant integrin ligand (50K) were stimulated with heparin-binding fragments of fibronectin (H/0) or a heparin-binding mutant (H/0-GAG) before fixation and staining for p190-A (green) and the lipid raft marker GM-1 (red). (A) Immunostaining of p190-A and GM-1, including masks used to measure the pixel intensity of the lamellar border. Bar, 5 µm. (B–E) Pixel intensity of p190-A (B and D) and GM-1 (C and E) within a 0.5-µm-thick border around the edge of each lamella after stimulation with H/0 (B and C) or H/0-GAG (D and E). The pixel intensity of 20 different cells was measured for each time point. The experiment was repeated on six separate occasions. Error bars represent standard error. *, significant change ($P < 10^{-8}$).

respectively (Fig. 1 F). The pattern of soluble p190-A levels in these lysates mirrored that observed with TrX lysates and included a significant increase in cytosolic p190-A at 30 min (Fig. 1 E). Changes in p190-A levels in the membrane pellets were more obvious, as, even at its peak, the amount of p190-A in the membrane pellet was lower than in the cytosolic fraction (Fig. 1 F), which indicates the presence of a large, nonmobile cytosolic pool. p190-A in the microsomal pellet peaked at 10 min and was followed by almost complete loss to the cytosol at 30 min (Fig. 1 E). The 10-min, membrane-bound peak was represented in the cytosolic analyses by a slight dip in soluble p190-A in sonication and TrX lysates, though it was less obvious, as it was partially masked by the nonmobile cytosolic pool.

In summary, the fractionation experiments reveal a biphasic redistribution of p190-A comprising membrane recruitment at 10 min followed by redistribution to the cytosol at 30 min, and can be compared with changes in RhoA activity in response to syndecan-4 engagement (Fig. 1 G). Membrane association of p190-A correlated closely with the reduction in RhoA activity immediately after H/0-stimulation, and both maxima and minima of the p190-A localization curve corresponded to the points of fastest change in RhoA activity. This relationship means that, in theory, RhoA regulation could be explained entirely in terms of p190-A localization during the first 45 min of syndecan-4 engagement. If the influences of all other GAPs and GEFs were ignored, a simple mathematical model based on the redistribution of p190-A would predict RhoA kinetics that precisely

Downloaded from http://rupress.org/jcb/article-pdf/181/6/1013/1551983/jcb_200711129.pdf by guest on 08 February 2026

match the experimental data. However, the reciprocal relationship breaks down over longer stimulation periods (Fig. 1 G and see Fig. 4 E), as levels of membrane-bound p190-A and active RhoA were both rising by 60 min, which indicates the involvement of alternative factors such as a Rho-GEF in sustained RhoA activity.

The redistribution of p190-A could be visualized by indirect immunofluorescence. Low levels of p190-A localization were seen in the lamellae of unstimulated cells, but this increased within 10 min of H/0 stimulation and was lost by 30 min (Fig. 2 A). The redistribution was quantified by measuring the pixel intensity of p190-A staining within a 0.5-μm-thick border around the edge of lamella (Fig. 2 B), yielding a pattern of redistribution that very closely resembled the biochemical data (Fig. 1 E). p190-A localization was unaffected by stimulation with the heparin-binding mutant H/0-GAG (Fig. 2 D). To control for nonspecific staining and reorganization of membrane compartments that might cause p190-A recruitment, cells were also stained with nonimmune IgG and for the lipid raft marker GM-1. Nonimmune staining did not change over the period of the experiment (unpublished data). Although there was partial overlap in p190-A and GM1 staining, the two did not colocalize extensively, and changes in GM-1 distribution, over time, followed a different pattern (Fig. 2 C); GM-1 was unaffected by H/0-GAG (Fig. 2 E). These differences suggest that the membrane association depends on modification of p190-A itself rather than membrane ruffling or the formation and dissolution of lipid rafts. Collectively, these data demonstrate that the engagement of syndecan-4 causes an initial recruitment of p190-A to the membrane at 10 min, followed by total displacement to the cytosol at 30 min before recovery by 90 min.

p190-A mediates RhoA regulation in response to engagement of syndecan-4

To test whether p190-A is indeed responsible for the syndecan-4–induced suppression of RhoA activity, we tested the kinetics of RhoA activity in p190-A knockout mouse embryonic fibroblasts (MEFs; Brouns et al., 2000). Wild-type MEFs exhibited a dip in RhoA activity in response to H/0 stimulation that recovered by 90 min (Fig. 3 A). This cycle took slightly longer to complete in MEFs than in the primary fibroblasts used in Fig. 1, which is consistent with the MEFs taking longer to form focal adhesions (see Fig. 4, D and E). The ability of H/0 to regulate RhoA was lost in the p190-A −/− MEFs (Fig. 3 B) but was restored by reexpression of p190-A to endogenous levels (Fig. 3, C and D). Disruption or reexpression of p190-A had no effect on the surface expression of either syndecan-4 or integrin subunits (Fig. S1, A–C, available at http://www.jcb.org/cgi/content/full/jcb.200711129/DC1). During the generation of the p190-A −/− MEFs, it was noted that the cells expressed a truncated version of p190-A (Brouns et al., 2000). The truncated protein lacked GAP activity but might retain some function or, more importantly, act as a dominant negative under certain circumstances. To ensure that the truncated protein was not responsible for the behavior of the p190-A −/− MEFs, H/0-dependent RhoA regulation was tested in MEFs transfected with an RNAi oligo

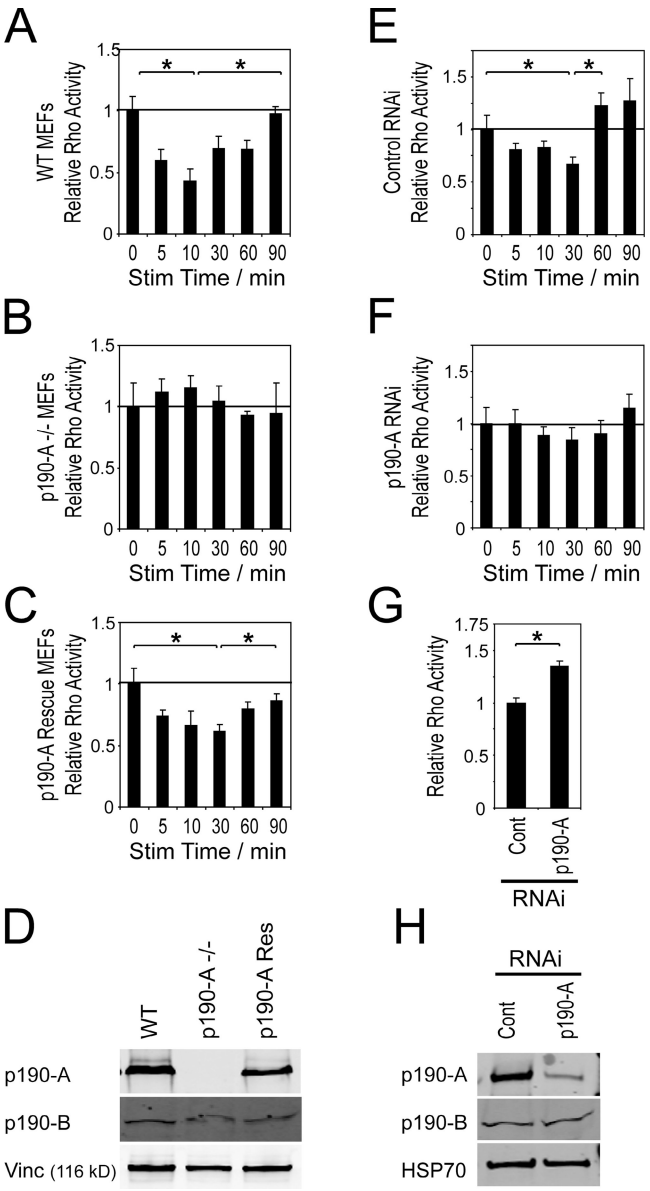

Figure 3. **p190-A mediates RhoA regulation in response to engagement of syndecan-4.** MEFs prespread on a recombinant integrin ligand (50K) were stimulated with heparin-binding fragments of fibronectin (H/0) before measuring the RhoA activity of lysates by ELISA. Wild-type MEFs (A), p190-A–null MEFs (B), p190-A–null MEFs reexpressing p190-A (C), MEFs transfected with a nontargeting siRNA (E), and MEFs transfected with an siRNA targeted against p190-A (F) are shown. (G) Direct comparison of RhoA activity in cells fully spread on 50K after transfection with a nontargeting or p190-A–targeted siRNA. (D and H) Expression levels of p190-A in null and reexpressing MEFs (D) or MEFs transfected with siRNAs (H); lysates were also probed for the related p190-B isoform to eliminate the possibility of molecular compensation or off-target knockdown. Equal loading between time points was confirmed by a total protein assay. Error bars represent standard error. *, significant change ($P < 0.05$) from experiments repeated on at least four separate occasions.

that reduced p190-A expression to <20% (Fig. 3 H). The addition of H/0 transiently suppressed RhoA activity in MEFs transfected with a nontargeting control oligo (Fig. 3 E) but had little effect on MEFs in which p190-A expression had been reduced (Fig. 3 F). Direct comparison of MEFs transfected with the two oligos revealed elevated RhoA activity in the cells with reduced

Downloaded from http://rupress.org/jcb/article-pdf/181/6/1013/1551983/jcb_200711129.pdf by guest on 08 February 2026

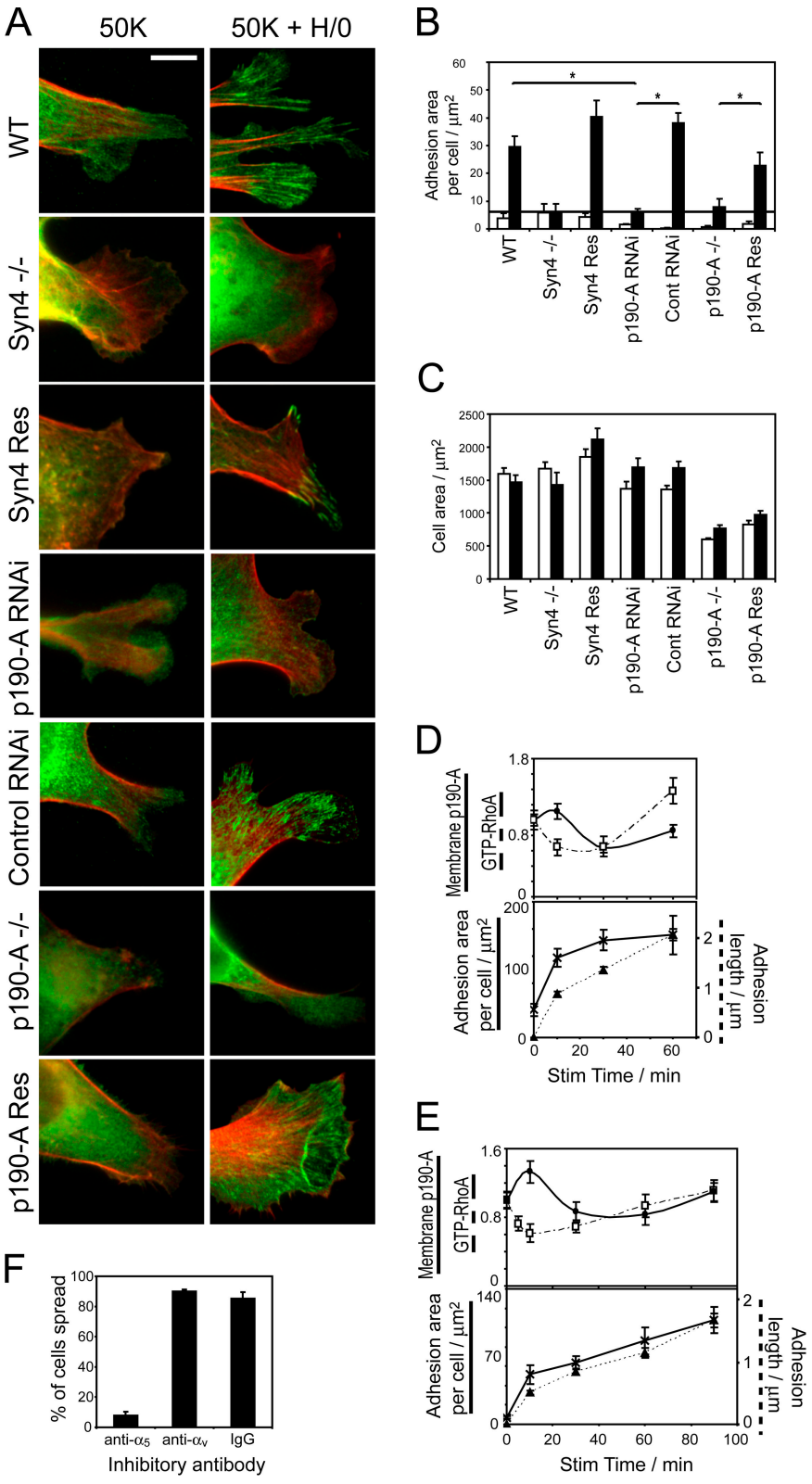

Figure 4. **Expression of p190-A is necessary for focal adhesion formation in response to syndecan-4 engagement.** (A) Wild-type, syndecan-4–null, siRNA-transfected, p190-A–null, or p190-A re-expressing MEFs prespread on a recombinant integrin ligand (50K) were stimulated with heparin-binding fragments of fibronectin (H/0) for 60 min before fixing and staining for vinculin (green) and/or actin (red). Whole cell images are shown in Fig. S2 A (available at http://www.jcb.org/cgi/content/full/jcb.200711129/DC1). Bar, 10 µm. (B) Focal adhesion area per cell was quantified digitally, after background subtraction, by measuring the area above an empirically determined threshold of fluorescence intensity within a single experiment. (C) Total area of individual cells. White bars represent cells spread on 50K and black bars represent spread cells after stimulation with H/0. (D and E) Correlation between membrane-bound p190-A (circles), RhoA activity (squares), total focal adhesion area per cell (crosses), and mean focal adhesion length (triangles) in human fibroblasts (D) and MEFs (E). (F) Percentage of human fibroblasts spread on 50K after 2 h in the presence of inhibitory antibodies against α_5 integrin (mAb16), α_v integrin (17E6), or nonimmune IgG. Experiments were repeated on four separate occasions. Error bars represent standard error. *, significant change ($P < 0.005$) from 20 cells per condition.

GAP expression (Fig. 3 G), and neither knockout nor knockdown of p190-A had any effect on the expression of the related B isoform of p190RhoGAP, which confirms that p190-A is a major determinant of RhoA activity in fibroblasts. These experiments, in combination with the correlation described in Fig. 1 G, demonstrate that the regulation of p190-A by membrane recruitment is responsible for the regulation of RhoA activity in response to syndecan engagement.

The connection between syndecan-4–induced RhoA regulation and focal adhesion formation was examined by immunostaining the different cell lines for vinculin-containing adhesion complexes after stimulation with integrin or syndecan-4 ligands.

Downloaded from http://rupress.org/jcb/article-pdf/181/6/1013/1551983/jcb_200711129.pdf by guest on 08 February 2026

Consistent with previous reports (Woods et al., 1986; Bloom et al., 1999; Bass et al., 2007b), wild-type MEFs only formed vinculin-containing focal adhesions upon engagement of both $\alpha_5\beta_1$ integrin and syndecan-4, whereas syndecan-4 −/− MEFs were incapable of forming focal adhesions even when stimulated with both ligands. p190-A −/− MEFs or MEFs in which p190 expression had been reduced by RNAi closely resembled the syndecan-4 −/− MEFs and failed to form focal adhesions in response to H/0, a defect that could be rescued by reexpression of p190-A (Figs. 4 A and S2 A, available at http://www.jcb.org/cgi/content/full/jcb.200711129/DC1). Focal adhesion formation was quantified by measuring the total adhesion area per cell using automated digital particle analysis. Only MEFs expressing both syndecan-4 and p190-A formed vinculin clusters above background level in response to H/0 (Fig. 4 B). Cell area was unaffected by expression of p190-A (Fig. 4 C), and although p190-A −/− MEFs were consistently smaller than wild-type MEFs, this appeared to be independent of p190-A, as reexpression failed to increase cell area and siRNA knockdown of p190-A had no effect on the cell area of wild-type MEFs. The kinetic correlation between RhoA activity and focal adhesion formation in response to H/0 was investigated by recording the dimensions of adhesion complexes over time. In primary fibroblasts stimulated with H/0, the total adhesion area increased rapidly as RhoA was inhibited ($t_{1/2}$ = 8.05 ± 2.86 min), which represents the initial formation of focal complexes (Figs. 4 D and S2 B). As RhoA was subsequently reactivated, the adhesions elongated until they resembled classical focal adhesions ($t_{1/2}$ = 32.4 ± 8.8 min). A similar correlation between RhoA activity and focal adhesion formation was observed in H/0-stimulated MEFs (Fig. 4 E). The phases of adhesion complex development in response to H/0 were further delineated by inhibiting signaling downstream of RhoA using Y27632 or C3 toxin. In the presence of inhibitors, H/0 induced the formation of punctate focal complexes that did not elongate over longer time periods, as RhoA could not be reactivated (Fig. S3). The time courses of adhesion complex formation and the failure of p190-deficient MEFs to form focal adhesions indicate that the formation of focal complexes during the suppression of RhoA activity is a critical stage in focal adhesion formation, and are consistent with previous findings that focal complex formation precedes the activation of RhoA during spreading on fibronectin (Nobes and Hall, 1995; Ren et al., 1999). However, as pharmacological inhibition of Rho was itself insufficient to induce focal complex formation, it is clear that the induction of other ECM-dependent signals such as Rac1 activation (Bass et al., 2007b) play an equally important role.

The dominant role of $\alpha_5\beta_1$ integrin, rather than $\alpha_v\beta_3$ integrin, as the receptor for 50K was confirmed by the application of inhibitory antibodies. A monoclonal antibody directed against α_5 integrin prevented spreading of human fibroblasts on 50K, whereas an antibody directed against α_v integrin or a nonimmune IgG had no effect (Fig. 4 F). The preferential use of a specific integrin during adhesion to fibronectin may be important, as β_1 and β_3 integrins have been found to have different effects on RhoA activity (Danen et al., 2002), and, so far, the potential for syndecan-4 to cooperate with $\alpha_v\beta_3$ integrin at the signaling or cell behavior levels has not been explored.

The focal adhesion formation defect of the p190-A −/− MEFs contrasted with previous findings that these cells organize their cytoskeleton normally when plated onto fibronectin (Brouns et al., 2000). We were able to reproduce focal adhesion formation by spreading p190-A −/− MEFs on whole fibronectin, and the similarity to the syndecan-4 −/− MEFs, which also form focal adhesions under these conditions, provides indirect support for a functional relationship between the molecules (Fig. S4, available at http://www.jcb.org/cgi/content/full/jcb.200711129/DC1). The ability of cells to compensate for the loss of syndecan-4 or p190-A under less stringent culture conditions implies a role for syndecan-4 in modulating the initial processes of ECM-dependent signaling. Both cell types overcome the short-term signaling deficiencies over longer time periods, which reflects the robust nature of eukaryotic cell signaling, but they respond to external stimuli less efficiently. This feature of ECM-dependent signaling goes some way to explaining the role of syndecan-4 in the rapid wound response but not development (Echtermeyer et al., 2001).

Together, these data suggest that p190-A provides a novel molecular link between syndecan-4 activity and the initial recruitment of cytoskeletal markers such as vinculin to focal adhesions due to inactivation of RhoA.

Syndecan-4 regulates p190-A localization through PKCα

The relocalization of p190-A in response to syndecan-4 engagement led us to investigate possible molecular connections from the adhesion receptor to the GTPase signal. Because syndecan-4 binds and activates PKCα (Koo et al., 2006), and phorbol ester–mediated PKC activation leads to phosphorylation of p190-A and membrane recruitment (Brouns et al., 2000), we tested whether the redistribution of p190-A, in response to H/0, required activation of PKCα by syndecan-4. Upon H/0 stimulation, p190-A redistributed into the TrX-soluble fractions of prespread MEFs with similar kinetics to the primary fibroblasts described in Fig. 1 (Fig. 5 A). In contrast, syndecan-4–null MEFs reexpressing a mutant syndecan-4 defective in PKCα binding (Y188L; Lim et al., 2003; Bass et al., 2007b) were incapable of redistributing p190-A (Fig. 5 B). Inhibition of PKC activity using a pharmacological inhibitor bisindolylmaleimide 1 (BIM-1; 200 nM) or reduction of PKCα expression to <10% by RNAi also blocked syndecan-4–dependent redistribution of p190-A, whereas transfection of MEFs with a nontargeting siRNA did not (Fig. 5, C–F). The influence of the PKCα-binding motif of syndecan-4 on the phosphorylation status of p190-A was measured directly by isotope labeling. MEFs expressing wild type or Y188L–syndecan-4 were metabolically labeled with [^{32}P]orthophosphate and spread on 50K before stimulation with H/0 for 10 min and immunoprecipitation of p190-A from cell lysates. Tyrosine phosphorylation of p190-A, measured by immunoblotting, was similar between wild-type and Y188L lines (Fig. 5 G). However, total phosphorylation, measured by isotope labeling, was reduced in Y188L–syndecan-4 MEFs (Fig. 5 H), which suggests that serine/threonine phosphorylation of p190-A is augmented by the direct activation of PKCα by syndecan-4. The residual phosphorylation of p190-A will be

Downloaded from http://rupress.org/jcb/article-pdf/181/6/1013/1551983/jcb_200711129.pdf by guest on 08 February 2026

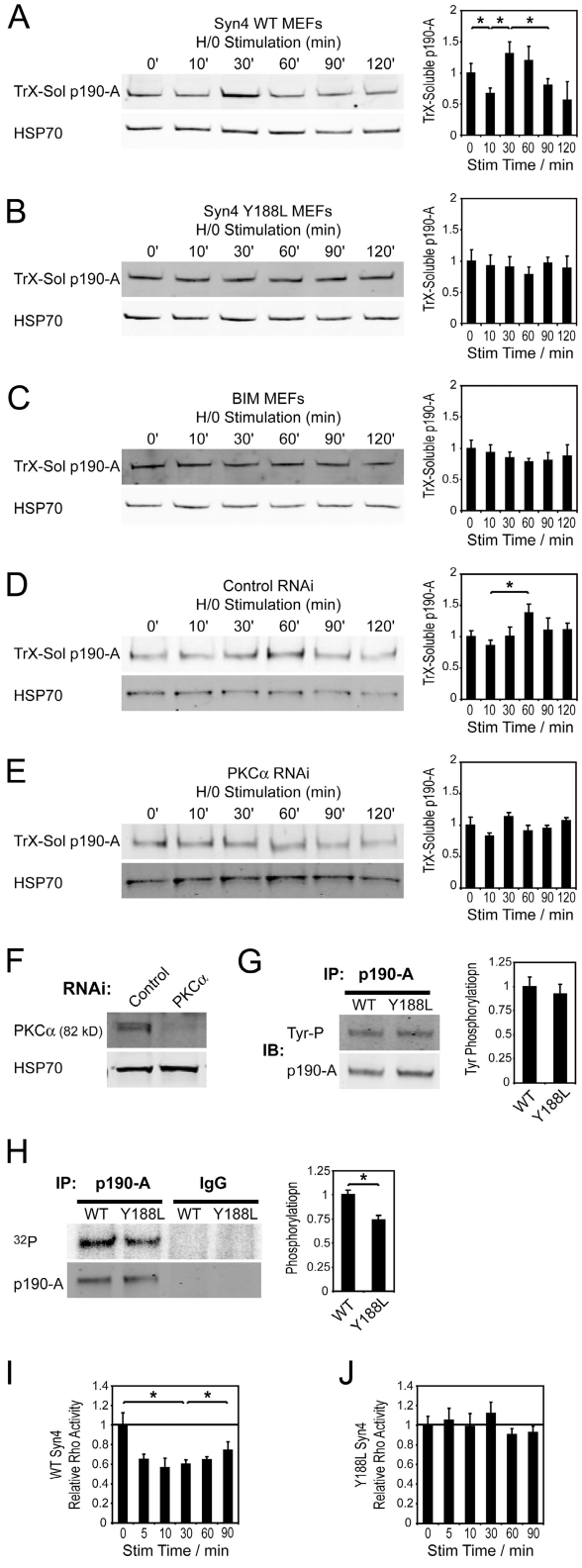

Figure 5. **PKCα mediates syndecan-4–induced redistribution of p190-A.** MEFs prespread on a recombinant integrin ligand (50K) were stimulated with heparin-binding fragments of fibronectin (H/0) before preparing lysates and then measuring levels of soluble p190-A in TrX lysates by Western blotting. Wild-type (A) and syndecan-4–null (B) MEFs reexpressing a Y188L mutant syndecan-4 defective in PKCα binding to endogenous levels, treated with 200 nM of the pharmacological PKC inhibitor BIM-1 (C), transfected with a nontargeting siRNA (D), and transfected with an siRNA targeted against PKCα (E). (F) Expression of PKCα after transfection with control or targeting siRNA. (G) Phosphotyrosine blots of p190-A immunoprecipitated from high-detergent lysates of MEFs expressing wild-type or Y188L-syndecan-4 spread on 50K and stimulated with H/0 for 10 min. (H) Phosphorimager scan and blot of p190-A immunoprecipitated from high-detergent lysates of MEFs expressing wild-type or Y188L–syndecan-4, metabolically labeled with [^{32}P]orthophosphate spread on 50K, and stimulated with H/0 for 10 min. RhoA activity ELISAs of MEFs expressing wild-type (I) or Y188L–syndecan-4 (J) prespread on 50K and stimulated with H/0. Equal loading between time points was confirmed by blotting for HSP70 or a total protein assay. Error bars represent standard error. *, significant change ($P < 0.05$) from experiments repeated on at least five separate occasions.

partly caused by tyrosine phosphorylation but might also include phosphorylation of other serine or threonine residues that is independent of syndecan-4. Finally, the effect of the PKCα-binding motif of syndecan-4 on RhoA regulation was assessed. H/0 stimulation triggered a wave of RhoA inhibition followed by reactivation in MEFs reexpressing wild-type syndecan-4 (Fig. 5 I) but had no effect on MEFs expressing the Y188L mutant (Fig. 5 J), demonstrating that the PKCα-binding motif of syndecan-4 is indeed responsible for the suppression of RhoA activity. We have shown previously that focal adhesion formation is blocked by the inhibition of PKCα (Bass et al., 2007b), and the fact that both suppression and reactivation of RhoA are compromised in Y188L–syndecan-4 MEFs indicates that RhoA activity is indeed held in balance by the localization of p190-A under the influence of PKCα. These experiments delineate a pathway from fibronectin to RhoA through syndecan-4, PKCα, and p190-A that would explain the suppression of RhoA activity at points of matrix contact.

$\alpha_5\beta_1$ integrin and syndecan-4 have distinct influences on p190-A

Most analyses of p190-A regulation have focused on the effect of adhesion-dependent tyrosine phosphorylation, which is necessary for p190-A activity (Arthur et al., 2000; Bradley et al., 2006). The cytoplasmic domains of syndecans associate with a Src-containing protein complex, and although there is no evidence that Src becomes activated by this association (Kinnunen et al., 1998), we examined whether syndecan-4 influenced the tyrosine phosphorylation status of p190-A in addition to regulating the PKCα pathway. The tyrosine phosphorylation status of p190-A, immunoprecipitated from lysates prepared in a high-detergent buffer, did not change in response to H/0 stimulation (Fig. 6 A). Tyrosine phosphorylation of p190-A from wild-type or Y188L–syndecan-4–expressing cells was also similar (Fig. 5 G), demonstrating that syndecan-4 was not itself responsible for the tyrosine phosphorylation. However, treatment of fibroblasts with the Src family kinase inhibitor PP2 (10 μM) blocked the redistribution of p190-A in response to H/0 (Fig. 6 B), demonstrating that Src family kinases, although not directly regulated by syndecan-4, are required for p190-A relocalization. This was confirmed by immunoprecipitation of p190-A from the membrane pellet, which showed enrichment of tyrosine-phosphorylated p190-A at the membrane when compared with p190-A immunoprecipitated from the soluble fraction (Fig. 6 C). The preferential redistribution of tyrosine-phosphorylated p190-A

Downloaded from http://rupress.org/jcb/article-pdf/181/6/1013/1551983/jcb_200711129.pdf by guest on 08 February 2026

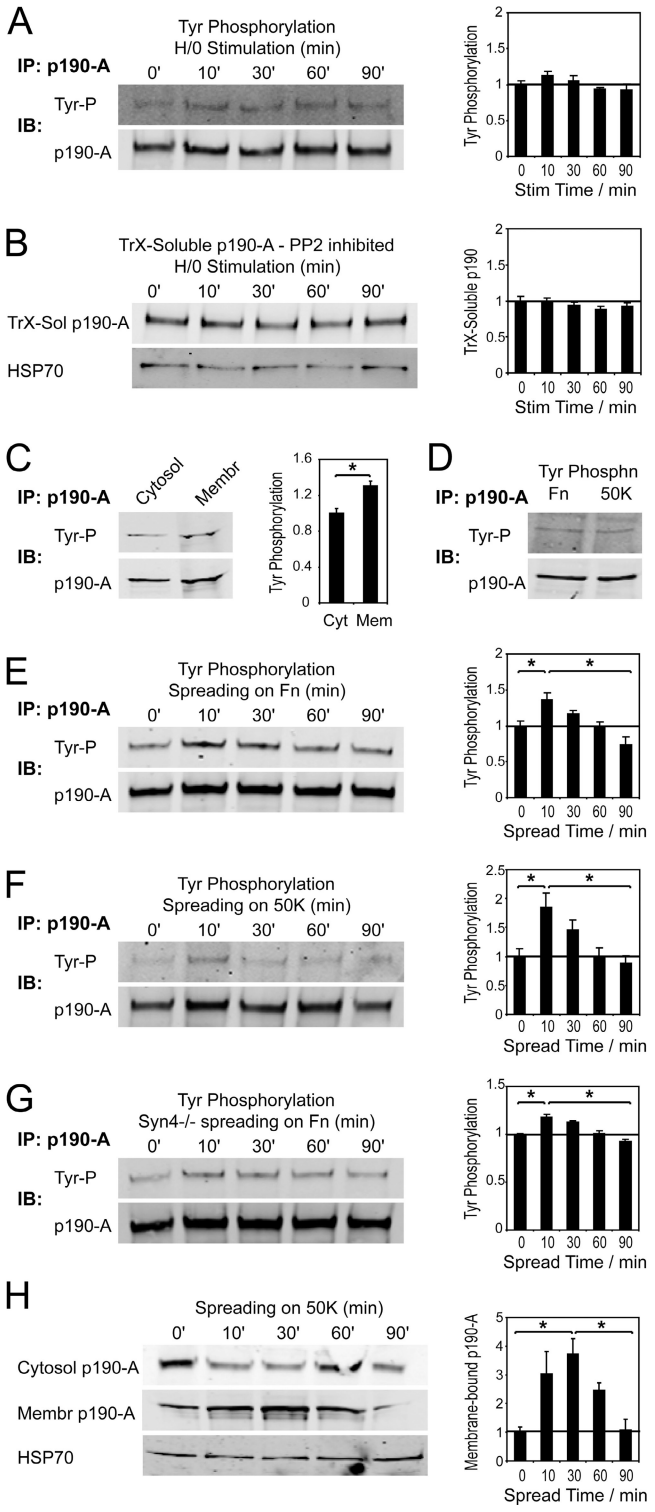

Figure 6. **$\alpha_5\beta_1$ integrin and syndecan-4 regulate p190-A by distinct mechanisms.** (A) Phosphotyrosine blots of p190-A immunoprecipitated from high-detergent lysates of fibroblasts prespread on 50K and stimulated with H/0. (B) TrX-soluble p190-A blots of fibroblasts prespread on 50K, inhibited with 10 μM PP2, and stimulated with H/0. (C) Phosphotyrosine blots of p190-A immunoprecipitated from the cytosolic and membrane-bound fractions of fibroblasts prespread on 50K, stimulated with H/0 for 10 min, and lysed by sonication. Loading was adjusted to analyze equal amounts of p190-A from each fraction. Phosphotyrosine blots of p190-A immunoprecipitated from high-detergent lysates of fibroblasts fully spread on fibronectin and 50K (D), spreading on fibronectin (E), spreading on 50K (F), or syndecan-4–null MEFs spreading on fibronectin (G). (H) Cytosolic and membrane-bound p190-A in sonication lysates of fibroblasts spreading on 50K. Equal loading between time points was confirmed by blotting for HSP70 in redistribution experiments and by reprobing blots for p190-A in tyrosine phosphorylation experiments. Error bars represent standard error. *, significant change ($P < 0.05$) from experiments repeated on at least four separate occasions.

explains why the 10-min dip of the 190-kD tyrosine-phosphorylated band in the TrX-soluble fraction (Fig. 1 A) is more apparent than the fall in total soluble p190-A (Fig. 1 C).

Because it has been found previously that tyrosine phosphorylation of p190-A increases during spreading on fibronectin (Arthur et al., 2000), and we found tyrosine phosphorylation to be a prerequisite of syndecan-4–dependent redistribution, the phosphorylation status of p190-A from cells spreading on an integrin-specific ligand was examined. The levels of tyrosine phosphorylation of p190-A from fibroblasts fully spread on 50K or fibronectin were similar (Fig. 6 D) and in agreement with previous studies (Arthur et al., 2000); p190-A immunoprecipitated from fibroblasts spreading on fibronectin was transiently tyrosine phosphorylated within 10–30 min (Fig. 6 E). A similar wave of phosphorylation was observed as cells spread on the integrin-specific ligand (50K; Fig. 6 F). Syndecan-4–null MEFs exhibited a similar peak in tyrosine phosphorylation of p190-A during spreading on fibronectin (Fig. 6 G), demonstrating that tyrosine phosphorylation of p190-A during spreading on fibronectin is indeed independent of syndecan-4. To test whether integrin engagement alone is capable of inducing redistribution of p190-A, cells spreading on 50K were lysed by sonication, and the membrane and cytosolic fractions were blotted for p190-A. Integrin engagement caused recruitment of p190-A to the membrane that coincided with elevated tyrosine phosphorylation (Fig. 6 H), which indicates that integrin and syndecan-4 each influence p190-A localization. Collectively, these experiments describe two discrete pathways from ECM receptor to p190-A (see Fig. 8 A): one from $\alpha_5\beta_1$ integrin to tyrosine kinase to p190-A that is entirely independent of syndecan-4 engagement and a second from syndecan-4 to PKCα to p190-A.

Signals from $\alpha_5\beta_1$ integrin and syndecan-4 combine to efficiently regulate RhoA

To resolve whether the parallel signals from $\alpha_5\beta_1$ integrin and syndecan-4 are both necessary for RhoA regulation, we examined the patterns of RhoA activity as cells spread on different ligands. MEFs spreading on fibronectin inhibited RhoA in a biphasic manner, with an initial rapid inactivation followed by a prolonged suppression until cells were fully spread (Fig. 7 A), which is characteristic of cells spreading in serum-free conditions (Ren et al., 1999). Although cells spreading on 50K were still capable of inhibiting RhoA, the initial, rapid suppression appeared to be compromised (Fig. 7 A). Similarly, syndecan-4–null MEFs spreading on fibronectin exhibited a defect in the first phase of RhoA signaling, confirming that the initial suppression is specific to syndecan-4 (Fig. 7 B). Strikingly, if the inhibitory effect of H/0 on RhoA in prespread MEFs was added to the inhibitory effect of 50K during cell spreading, the resultant curve closely resembled the curve seen upon engagement of both $\alpha_5\beta_1$

Downloaded from http://rupress.org/jcb/article-pdf/181/6/1013/1551983/jcb_200711129.pdf by guest on 08 February 2026

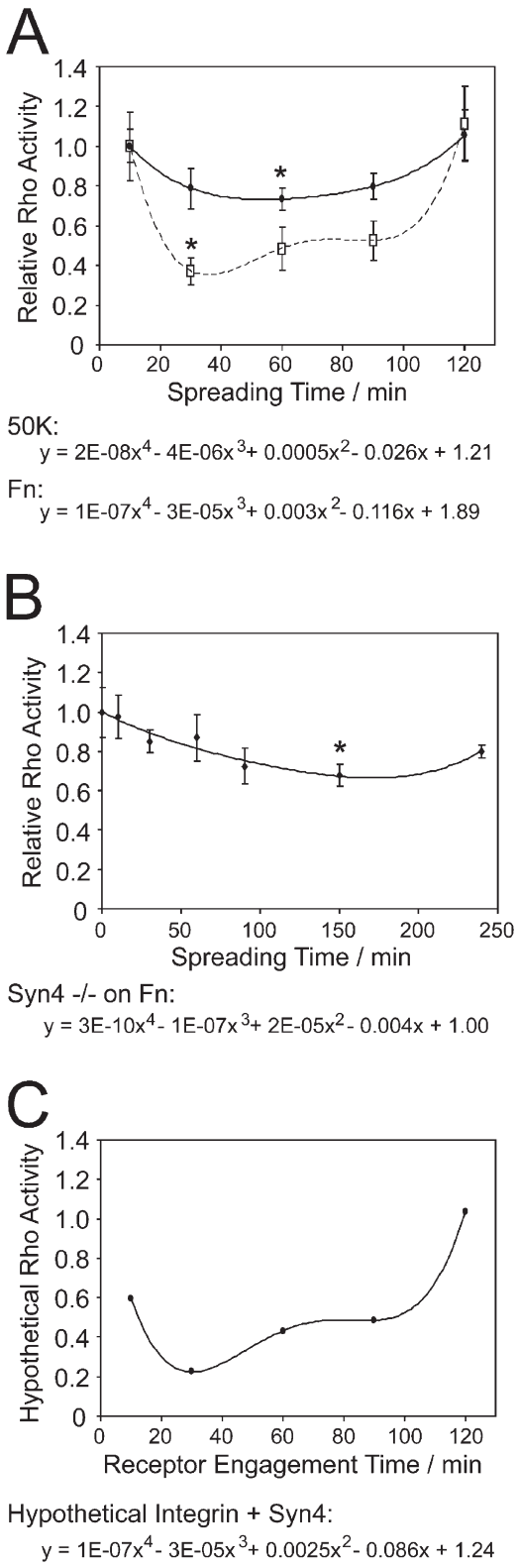

Figure 7. **Engagement of $\alpha_5\beta_1$ integrin and syndecan-4 each contribute to efficient suppression of RhoA during spreading on fibronectin.** (A) Rho-A activity of MEFs spreading on fibronectin (broken line) or 50K (solid line) measured by ELISA. (B) RhoA activity of syndecan-4–null MEFs spreading on fibronectin. (C) Hypothetical RhoA activity calculated by adding the percentage suppression caused by H/0 on prespread cells to the suppression caused during spreading on 50K. Fourth-order polynomial curves were fitted to each dataset. Experiments were repeated on at six separate occasions. Equal loading between time points was confirmed by a total protein assay. Error bars represent standard error. *, significant change from initial activity ($P < 0.05$).

integrin and syndecan-4 by fibronectin (Fig. 7, A and C). The result of combining mathematically the effects of $\alpha_5\beta_1$ integrin and syndecan-4 on RhoA activity reflects the cumulative effects of $\alpha_5\beta_1$ integrin and syndecan-4 on membrane recruitment of p190-A through the tyrosine and serine/threonine phosphorylation mechanisms, respectively. A fourth-order polynomial curve fitted to the hypothetical data described kinetics that were almost identical to those obtained experimentally during spreading on fibronectin (Fig. 7 C) and led us to conclude that not only is p190-A the convergence point for signals from independent adhesion receptors, but that engagement of both receptors is necessary to achieve the efficient regulation of RhoA observed during spreading on fibronectin.

Discussion

In this paper, our major finding is that independent protein kinase pathways downstream of $\alpha_5\beta_1$ integrin and syndecan-4 converge on p190-A and are necessary for efficient regulation of RhoA (Fig. 8 A). We identify a linear connection from syndecan-4 to the redistribution of p190-A, via PKCα, that is responsible for the initial phase of RhoA suppression during cell spreading. We also find that signaling via p190-A is necessary for the H/0-induced formation of vinculin-containing focal adhesions. ECM-dependent tyrosine phosphorylation of p190-A occurs independently of syndecan-4 but primes p190-A for H/0-induced redistribution and also causes a second, integrin-dependent wave of membrane recruitment that allows the sustained suppression of RhoA until a cell is fully spread. The differences in the contributions of $\alpha_5\beta_1$ integrin (essential) and syndecan-4 (modulatory) to p190-A regulation explain why cells spread on 50K but not H/0 alone and, more importantly, how receptor cooperation regulates efficient membrane protrusion and adhesion formation during cell migration.

Cell migration requires that the leading edge undergoes cycles of membrane protrusion, attachment, and cytoskeletal contraction, which causes translocation (Giannone et al., 2007), and this necessitates the alternate activation of Rac1 and RhoA in the lamellipodium. Fluorescence resonance energy transfer biosensors have revealed that both Rac1 and RhoA are active at the edge of a lamellipodium (Itoh et al., 2002; Pertz et al., 2006) and must be regulated very rapidly. In vivo, a cell is constitutively associated with the ECM across its surface, which means that if engagement of a single receptor was sufficient for regulation of GTPase activity, it would be impossible to restrict GTPase regulation to the leading edge. However, localized signaling can be easily explained in the context of a pair of coupled ECM receptors. The "anchoring receptor" (e.g., integrin) links the cell to its environment, regulates long-term signaling events, and permits signaling by the "sensory receptor" (e.g., syndecan-4), which regulates GTPases rapidly upon de novo ECM engagement at the leading edge and causes a cell to migrate toward exposed matrix. Syndecan-4 is ideally suited to act as the ECM sensor.

Downloaded from http://rupress.org/jcb/article-pdf/181/6/1013/1551983/jcb_200711129.pdf by guest on 08 February 2026

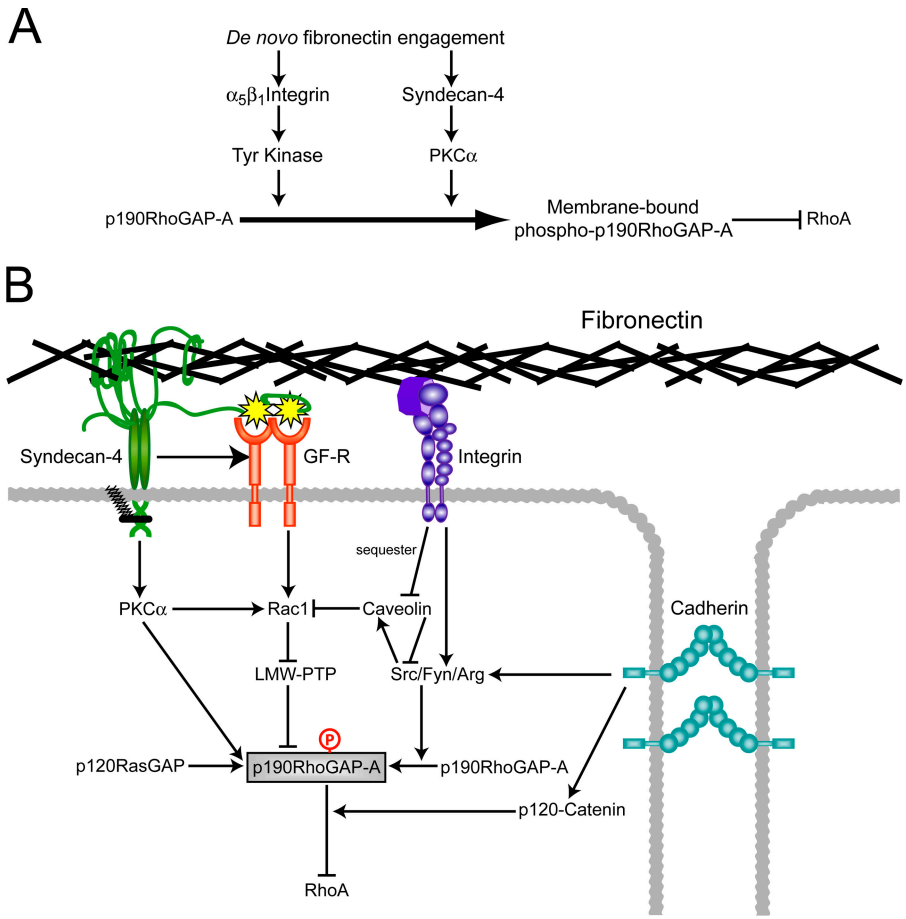

Figure 8. **The network of signals arising from transmembrane receptor engagement converge on p190-A.** (A) Summary of the connections from $\alpha_5\beta_1$ integrin and syndecan-4 during the initiation of focal adhesion formation. (B) The engagement of receptors, including integrins and cadherins, results in tyrosine phosphorylation of p190-A (gray box). The primed p190-A molecule is itself a target for serine and threonine phosphorylation events, tyrosine dephosphorylation events downstream of syndecan-4 and growth factor receptors, and trafficking molecules such as p120RasGAP. Although there is extensive crosstalk between these pathways, p190-A stands out as a nexus for the multiple signaling events during RhoA regulation.

The large, flexible glycosaminoglycan chains, through which syndecans engage the full spectrum of ECM molecules, can project up to 500 nm from the cell surface (Weinbaum et al., 2007) compared with the 16-nm reach of integrins (Takagi et al., 2001), and are capable of binding ligands that are dilute or distant from the cell membrane. A consequence of the synergy model is that cell migration depends on two key signaling axes: divergence of signals from adhesion receptors to both Rac1 and RhoA (Bass et al., 2007b; Dovas et al., 2006) and convergence of signals from $\alpha_5\beta_1$ integrin and syndecan-4 on Rac1 (Bass et al., 2007b; Del Pozo et al., 2004) and p190-A, as described here. It is worth noting that the peak in membrane-bound p190-A and the dip in RhoA activity (Fig. 1 G) coincide with the peak in H/0-induced Rac1 activity in the same cell type (Bass et al., 2007b), and it is logical that regulation of the antagonistic actions of Rac1 and RhoA should stem from the same pair of receptors. The involvement of coupled ECM receptors not only explains how coordinated signaling can be achieved, but also why the molecular link from adhesion receptor to GTPase has proven so difficult to resolve.

This model of signal convergence can in theory be expanded to incorporate the influences of other transmembrane receptors. The antagonistic relationship between Rac1 and RhoA, which is also influenced by growth factor receptor signaling, involves indirect inhibition of low–molecular weight protein tyrosine phosphatase by Rac1 and results in elevated tyrosine phosphorylation of p190-A (Fig. 8 B, center; Nimnual et al., 2003). The glycosaminoglycan chains of syndecans themselves contribute to growth factor signaling by capturing and presenting growth factors to specific receptors (Bernfield et al., 1999), whereas Rac1 activation and cell migration in response to FGF depend on an intact syndecan-4 cytoplasmic domain (Tkachenko et al., 2006) and may be representative of a broader cooperation between growth factor receptors and syndecan-4 (Fig. 8 B, left). Links have also been drawn to p190-A from the cadherin family of cell–cell receptors (Wildenberg et al., 2006). Like the integrin pathway, engagement of cadherin induced tyrosine phosphorylation of p190-A (Noren et al., 2003) and recruitment to the membrane by direct association between p190-A and p120-catenin (Fig. 8 B, right; Wildenberg et al., 2006). This concept is particularly important, as cell–cell and cell–matrix interactions have opposing influences on cell migration and proliferation that must be linked mechanistically.

The most explicit demonstrations of the central role of p190-A in cell signaling have been the correlation between increased tyrosine phosphorylation of p190-A and disassembly of actin stress fibers in v-Src–transformed fibroblasts, and the ability to block v-Src transformation with a GAP-insensitive mutant of RhoA (Fincham et al., 1999). Although phosphorylation by Src has been shown to augment the in vitro GAP activity of p190-A (Arthur et al., 2000), the activity of p190-A is largely dependent on localization. Phosphorylation of tyrosine-1105 of p190-A by Src, Fyn, or Arg causes association with the SH2 domains of p120RasGAP (Roof et al., 1998; Bradley et al., 2006)

Downloaded from http://rupress.org/jcb/article-pdf/181/6/1013/1551983/jcb_200711129.pdf by guest on 08 February 2026

and is necessary for the suppression of RhoA during spreading on fibronectin (Bradley et al., 2006). Unlike the Src pathway, neither phosphorylation by Arg nor association with p120RasGAP are thought to affect the GAP activity of p190-A in vitro, and this may represent differences in uncharacterized phosphorylation or scaffolding events downstream of either Src or Arg. It is clear that the interaction between p120RasGAP and tyrosine-phosphorylated p190-A is essential for the recruitment of p190-A to the cell periphery, possibly via the pleckstrin homology and phospholipid-binding domains of p120RasGAP (Bradley et al., 2006). Evidence for compromised p190-A function upon membrane modification comes from disruption of the cholesterol-rich membrane microdomain component caveolin-1 (Grande-Garcia et al., 2007). Caveolin-1–null fibroblasts exhibited reduced RhoA activity and a loss of persistent migration that was a consequence of increased Src activity and mediated by p190-A. Likewise, knockdown of the caveolin-binding protein filamin prevented redistribution of p190-A between membrane fractions and, as a consequence, regulation of RhoA activity (Mammoto et al., 2007). Notably, caveolin-1 activity also inhibited Rac1 by internalizing cholesterol-rich microdomains that were necessary for signaling downstream of Rac1, providing a further antagonistic link to both Rac1 and RhoA (Del Pozo et al., 2005). Collectively, these reports indicate that membrane recruitment of p190-A is the critical determinant of RhoA activity. Our data expand this model by identifying syndecan-4 as a regulator of p190-A localization that exerts its effect through PKCα. By isolating the tyrosine kinase–mediated redistribution of p190-A, which is downstream of integrins from the syndecan-4 signal, and finding that both events are necessary for the biphasic regulation of RhoA during cell spreading, we identify p190-A as a key nodal point in ECM-dependent signaling.

Materials and methods

Antibodies and reagents

Mouse monoclonal antibodies raised against p190-A and phosphotyrosine (4G10; Millipore), vinculin (Sigma-Aldrich), HSP70 (Affinity BioReagents), PKCα (BD Biosciences), and transferrin receptor (Invitrogen); a rat monoclonal antibody against TCP-1α (Assay Designs); and a rabbit polyclonal antibody against p190-B (Cell Signaling Technology) were used according to the manufacturer's instructions. Cy2-conjugated anti–mouse IgG was obtained from Jackson ImmunoResearch Laboratories, Alexa Fluor 680–conjugated anti–mouse IgG and TRITC-conjugated phalloidin were obtained from Invitrogen, and FITC-conjugated cholera toxin subunit B for GM-1 staining was obtained from Sigma-Aldrich. Recombinant fibronectin polypeptides encompassing type III repeats 6–10 (50K), 12–15 (H/0), and 12–14 substituted at the heparin-binding motifs (H/0-GAG) were expressed as recombinant polypeptides as described previously (Makarem et al., 1994), and bovine plasma fibronectin was obtained from Sigma-Aldrich. Inhibitory integrin antibodies against human α_5 (mAb16) or human α_v (17E6) were gifts from K. Yamada (National Institutes of Health, Bethesda, MD) and S. Goodman (Merck, Darmstadt, Germany), respectively.

Cell culture

The generation of immortalized wild-type, syndecan-4 −/−, and Y188L–syndecan-4–expressing MEFs has been described previously (Bass et al., 2007b). To allow expression of the large T antigen, the MEFs were cultured at 33°C in DME (Sigma-Aldrich) supplemented with 10% fetal bovine serum, 2 mM L-glutamine, and 20 U/ml IFNγ (Sigma-Aldrich). p190-A −/− MEFs were cultured in DME supplemented with 10% fetal bovine serum, 2 mM L-glutamine, 1% (vol/vol) penicillin, and streptomycin. p190-A was reexpressed by infecting null cells with p190-A–encoding virions harvested from transfected AM-12 retroviral packaging cells. Primary human foreskin fibroblasts, passage number 8–25, were cultured at 37°C in DME supplemented with 10% fetal bovine serum, 4.5 g/liter glucose, 1 mM sodium pyruvate, 2 mM L-glutamine, 0.1 mM nonessential amino acids, MEM vitamins, and 20 µg/ml gentamycin. 1–2 d before each experiment, cells were passaged to ensure an active proliferative state.

Cell spreading and adhesion complex formation assays

For immunofluorescence, 13-mm-diameter glass coverslips were derivatized for 30 min with 1 mM sulpho-m-maleimidobenzoyl-*N*-hydrosuccinimide ester (Thermo Fisher Scientific). For biochemical assays, 9-cm tissue culture–treated plastic dishes (Corning) were coated directly with ligand. Coverslips or dishes were coated for 2 h at room temperature with 10 µg/ml fibronectin polypeptides in Dulbecco's PBS containing calcium and magnesium (BioWhittaker) and blocked with 10 mg/ml heat-denatured BSA for 30 min at room temperature (Humphries et al., 1986). Equivalent ligand coating between glass and plastic was tested by ELISA using the anti-fibronectin mAb 333 (Bass et al., 2007a). To prevent de novo synthesis of ECM and other syndecan-4 ligands, cells were treated with 25 µg/ml cycloheximide (Sigma-Aldrich) for 2 h before detachment (Couchman et al., 1983) and then detached with 0.5 mg/ml trypsin. Cells were resuspended in DME and 25 µg/ml cycloheximide, plated at a density of 1.25×10^4 cells per coverslip or 10^6 cells per dish, and allowed to spread at 37°C for 2 h for H/0 stimulation experiments or the appropriate time periods for spreading assays. Prespread cells were treated with pharmacological inhibitors (200 nM BIM-1 [EMD], 10 µM PP2 [EMD], 10 µM Y27632 [EMD], and 2 µg/ml membrane-permeable C3 toxin [Tebu-Bio]) for 30 min if appropriate, and then stimulated with 10 µg/ml H/0 or H/0-GAG with or without pharmacological inhibitors for 0–120 min before fixing or preparing lysates. Stimuli were added at staggered intervals to maintain a consistent, 4-h period between plating and fixation or lysis. For immunofluorescence, cells were fixed with 4% (wt/vol) paraformaldehyde, permeabilized with 0.5% (wt/vol) TrX diluted in PBS, and blocked with 3% (wt/vol) BSA in PBS. Fixed cells were stained for p190-A, GM-1, vinculin, or actin; mounted in Prolong Antifade (Invitrogen); and photographed on a microscope system (DeltavisionRT; Deltavision) using a 100× NA 1.35 UPlan Apo objective (Olympus) and a camera (CH350; Roper Scientific). Images were compiled and analyzed using ImageJ software. The total area of adhesion complexes per cell was calculated by recording automatically the area of fluorescence intensity above an empirically determined threshold after rolling ball background subtraction. The same threshold was used for all conditions within a single experiment. The lengths of individual focal ahesions were measured manually. Estimates of the half-times of adhesion maturation were calculated by fitting a 3-parameter hyperbola to the measurements of focal area or length. The intensity of p190-A and GM-1 staining at the periphery of a cell was measured by manually drawing a border, 0.5-µm wide, around the lamellae of cells to create a set of masks and then measuring the mean pixel intensity of unadjusted images within the defined area.

Preparation of lysates

All lysates were prepared at 4°C from spread cells that had been washed with ice-cold PBS by scraping cells in the appropriate lysis buffer containing 0.5 mM AEBSF, 25 µg/ml aprotinin, 25 µg/ml leupeptin, 5 mM Na_2VO_4, and 10 mM NaF. For membrane fractionation by partial TrX lysis, we used 50 mM Tris-Cl, pH 7.5, 150 mM NaCl, 0.5% (vol/vol) TrX, 10 mM $MgCl_2$, and 5 mM EGTA, and lysates were clarified at 22,000 *g*. For membrane fractionation by sonication, cells were scraped in Dulbecco's PBS containing calcium and magnesium (BioWhittaker) and lysed by three 5-s 20% pulses using a sonicator (Vibra-Cell; Sonics & Materials, Inc.). Nuclear debris was then removed with a 7 min, 1,000 *g* centrifugation step, and membrane-bound material was harvested at 22,000 *g* for a further 7 min. Harsh detergent lysates for immunoprecipitation were prepared in 50 mM Tris-Cl, pH 7.5, 150 mM NaCl, 1% (vol/vol) TrX, 0.5% (wt/vol) sodium deoxycholate, 0.1% (wt/vol) sodium dodecyl sulfate, 10 mM $MgCl_2$, and 5 mM EGTA, and clarified at 4,000 *g* before preclearing for 30 min with protein G–Sepharose (Invitrogen). p190-A was then affinity purified for 2 h using 1 µg of monoclonal antibody and protein G–Sepharose. For immunoprecipitation from the fractionated membrane pellet, the pellet was resuspended in the harsh detergent buffer by three 5-s 20% somincator pulses. Proteins from all experiments were solubilized in SDS sample buffer, resolved by SDS-PAGE, and transferred to nitrocellulose. Transferred proteins were detected using the Odyssey Western blotting fluorescent detection system (LI-COR Biosciences UK Ltd.). This involved blocking the membranes with casein blocking buffer (Sigma-Aldrich) and then incubating with the primary antibodies diluted 1:1,000 in blocking buffer and

Downloaded from http://rupress.org/jcb/article-pdf/181/6/1013/1551983/jcb_200711129.pdf by guest on 08 February 2026

0.1% (vol/vol) Tween-20. Membranes were washed with PBS and 0.1% (vol/vol) Tween-20, and incubated with Alexa Fluor 680–conjugated anti–mouse IgG diluted 1:5,000 in blocking buffer and 0.1% (vol/vol) Tween-20. After rinsing the membrane, proteins were detected using an infrared imaging system that allowed both an image of the membrane and an accurate count of bound protein to be recorded. For all experiments, equivalent loading between time points was confirmed by blotting the crude lysate for either HSP70 or vinculin. The significance of changes in abundance was established using paired Student's *t* tests of normally distributed small samples ($n = 4–8$).

Rho activity ELISA

A commercially available Rho ELISA assay was obtained from Tebu-Bio and used according to manufacturer's instructions. In brief, this involved capturing GTP-RhoA from clarified cell lysate in a 96-well plate coated with the Rho-binding domain of rhotekin. Captured RhoA was then cross-linked to the plate and detected by sequential incubations with an anti-RhoA primary antibody and an HRP-conjugated secondary antibody. The relative amount of bound RhoA was then measured by developing the plate with an HRP-sensitive dye, stopping development with dilute sulfuric acid, and recording absorbance at 490 nm using a multiscan plate reader. Initial lysis steps were performed on ice and completed within 10 min to limit hydrolysis of bound GTP.

Metabolic labeling

MEFs expressing wild-type or Y188L mutant syndecan-4 were starved of phosphate and serum for 2 h during incubation with cycloheximide. Phosphate-depleted cells were trypsinized, and 8×10^5 cells were spread in 50K-coated, 25-cm^2 flasks in serum-free, phosphate-free media (Invitrogen) containing 0.3 mCi/ml [^{32}P]orthophosphate (PerkinElmer) for 2.5 h. Spread cells were stimulated with 10 µg/ml H/0 for 10 min before lysis in 50 mM Tris-HCl, pH 7.5, 150 mM NaCl, 1% (vol/vol) TrX, 0.5% (wt/vol) sodium deoxycholate, 0.1% (wt/vol) sodium dodecyl sulfate, 10 mM $MgCl_2$, 5 mM EGTA, 0.5 mM AEBSF, 25 µg/ml aprotinin, 25 µg/ml leupeptin, 5 mM Na_2VO_4, 10 mM NaF, and 1× phosphatase inhibitor cocktail 1 (Sigma-Aldrich). Clarified lysates were precleared for 30 min with protein G–Sepharose (Invitrogen) and nonimmune rat IgG before immunoprecipitating the p190-A using 1 µg of monoclonal antibody and protein G–Sepharose. Proteins were solubilized in SDS sample buffer and resolved by reducing SDS-PAGE. Dried PAGE gels were exposed to a phosphorimager screen overnight and scanned using a multi-imaging system (Molecular Imager FX; Bio-Rad Laboratories).

RNAi knockdown of PKCα and p190-A

siRNA duplexes targeting mouse PKCα sequences (sense) 5′-GAAGGGUUCUCGUAUGUCAUU-3′ or 5′-UAACAUAGACCAAUCUGAUUU-3′, a mouse p190-A sequence (sense) 5′-UAGUGCAACUCAUUGAUAAUU-3′ (with ON TARGET modification for enhanced specificity), and an siGLO, nontargetting control duplex were obtained from Thermo Fisher Scientific. For knockdown of PKCα, 0.8 nmol of oligo was transfected into a 90%-confluent 75-cm^2 flask of wild-type MEFs using Lipofectamine 2000 reagent (Invitrogen). After 24 h, the cells were passaged and then used for experiments after a further 24 h. For knockdown of p190-A, 1 nmol of oligo was transfected every 2–3 d, and suitable knockdown was achieved after at least 8 d of this regimen. Expression of PKCα or p190-A was tested by Western blotting.

Online supplemental material

Fig. S1 shows flow cytometric analysis of integrin and syndecan expression, and Western analysis of p190-A expression in transgenic cell lines. Fig. S2 shows images of vinculin-stained cells after H/0 stimulation to complement Fig. 4. Fig. S3 shows the effects of Y27632 and C3 on H/0-induced focal adhesion formation. Fig. S4 shows images and focal adhesion quantification of syndecan-4 and p190-A–null MEFs spread on fibronectin. Online supplemental material is available at http://www.jcb.org/cgi/content/full/jcb.200711129/DC1.

We would like to thank Charles Streuli for critical reading of the manuscript.

This work was supported by grants 045225 and 074941 from the Wellcome Trust (to M.J. Humphries). The Bioimaging Facility microscopes used in this study were purchased with grants from the Biotechnology and Biological Sciences Research Council, the Wellcome Trust, and the University of Manchester Strategic Fund.

Submitted: 26 November 2007
Accepted: 16 May 2008

References

Arias-Salgado, E.G., S. Lizano, S.J. Shattil, and M.H. Ginsberg. 2005. Specification of the direction of adhesive signaling by the integrin beta cytoplasmic domain. *J. Biol. Chem.* 280:29699–29707.

Arnaout, M.A., B. Mahalingam, and J.P. Xiong. 2005. Integrin structure, allostery, and bidirectional signaling. *Annu. Rev. Cell Dev. Biol.* 21:381–410.

Arthur, W.T., and K. Burridge. 2001. RhoA inactivation by p190RhoGAP regulates cell spreading and migration by promoting membrane protrusion and polarity. *Mol. Biol. Cell.* 12:2711–2720.

Arthur, W.T., L.A. Petch, and K. Burridge. 2000. Integrin engagement suppresses RhoA activity via a c-Src-dependent mechanism. *Curr. Biol.* 10:719–722.

Bass, M.D., M.R. Morgan, and M.J. Humphries. 2007a. Integrins and syndecan-4 make distinct, but critical, contributions to adhesion contact formation. *Soft Matter.* 3:372–376.

Bass, M.D., K.A. Roach, M.R. Morgan, Z. Mostafavi-Pour, T. Schoen, T. Muramatsu, U. Mayer, C. Ballestrem, J.P. Spatz, and M.J. Humphries. 2007b. Syndecan-4–dependent Rac1 regulation determines directional migration in response to the extracellular matrix. *J. Cell Biol.* 177:527–538.

Bernfield, M., M. Gotte, P.W. Park, O. Reizes, M.L. Fitzgerald, J. Lincecum, and M. Zako. 1999. Functions of cell surface heparan sulfate proteoglycans. *Annu. Rev. Biochem.* 68:729–777.

Bloom, L., K.C. Ingham, and R.O. Hynes. 1999. Fibronectin regulates assembly of actin filaments and focal contacts in cultured cells via the heparin-binding site in repeat III13. *Mol. Biol. Cell.* 10:1521–1536.

Bradley, W.D., S.E. Hernandez, J. Settleman, and A.J. Koleske. 2006. Integrin signaling through Arg activates p190RhoGAP by promoting its binding to p120RasGAP and recruitment to the membrane. *Mol. Biol. Cell.* 17:4827–4836.

Brouns, M.R., S.F. Matheson, K.Q. Hu, I. Delalle, V.S. Caviness, J. Silver, R.T. Bronson, and J. Settleman. 2000. The adhesion signaling molecule p190 RhoGAP is required for morphogenetic processes in neural development. *Development.* 127:4891–4903.

Burridge, K., and K. Wennerberg. 2004. Rho and Rac take center stage. *Cell.* 116:167–179.

Cavani, A., G. Zambruno, A. Marconi, V. Manca, M. Marchetti, and A. Giannetti. 1993. Distinctive integrin expression in the newly forming epidermis during wound healing in humans. *J. Invest. Dermatol.* 101:600–604.

Chakravarti, R., and J.C. Adams. 2006. Comparative genomics of the syndecans defines an ancestral genomic context associated with matrilins in vertebrates. *BMC Genomics.* 7:83.

Couchman, J.R., M. Hook, D.A. Rees, and R. Timpl. 1983. Adhesion, growth, and matrix production by fibroblasts on laminin substrates. *J. Cell Biol.* 96:177–183.

Danen, E.H., S. Aota, A.A. van Kraats, K.M. Yamada, D.J. Ruiter, and G.N. van Muijen. 1995. Requirement for the synergy site for cell adhesion to fibronectin depends on the activation state of integrin alpha 5 beta 1. *J. Biol. Chem.* 270:21612–21618.

Danen, E.H., P. Sonneveld, C. Brakebusch, R. Fassler, and A. Sonnenberg. 2002. The fibronectin-binding integrins α5β1 and αvβ3 differentially modulate RhoA-GTP loading, organization of cell matrix adhesions, and fibronectin fibrillogenesis. *J. Cell Biol.* 159:1071–1086.

Del Pozo, M.A., N.B. Alderson, W.B. Kiosses, H.H. Chiang, R.G. Anderson, and M.A. Schwartz. 2004. Integrins regulate Rac targeting by internalization of membrane domains. *Science.* 303:839–842.

Del Pozo, M.A., N. Balasubramanian, N.B. Alderson, W.B. Kiosses, A. Grande-Garcia, R.G. Anderson, and M.A. Schwartz. 2005. Phospho-caveolin-1 mediates integrin-regulated membrane domain internalization. *Nat. Cell Biol.* 7:901–908.

Dovas, A., A. Yoneda, and J.R. Couchman. 2006. PKCbeta-dependent activation of RhoA by syndecan-4 during focal adhesion formation. *J. Cell Sci.* 119:2837–2846.

Echtermeyer, F., M. Streit, S. Wilcox-Adelman, S. Saoncella, F. Denhez, M. Detmar, and P. Goetinck. 2001. Delayed wound repair and impaired angiogenesis in mice lacking syndecan-4. *J. Clin. Invest.* 107:R9–R14.

Fincham, V.J., A. Chudleigh, and M.C. Frame. 1999. Regulation of p190 RhoGAP by v-Src is linked to cytoskeletal disruption during transformation. *J. Cell Sci.* 112:947–956.

Gallo, R., C. Kim, R. Kokenyesi, N.S. Adzick, and M. Bernfield. 1996. Syndecans-1 and -4 are induced during wound repair of neonatal but not fetal skin. *J. Invest. Dermatol.* 107:676–683.

Giannone, G., B.J. Dubin-Thaler, O. Rossier, Y. Cai, O. Chaga, G. Jiang, W. Beaver, H.G. Dobereiner, Y. Freund, G. Borisy, and M.P. Sheetz. 2007. Lamellipodial actin mechanically links myosin activity with adhesion-site formation. *Cell.* 128:561–575.

Grande-Garcia, A., A. Echarri, J. de Rooij, N.B. Alderson, C.M. Waterman-Storer, J.M. Valdivielso, and M.A. del Pozo. 2007. Caveolin-1 regulates

Downloaded from http://rupress.org/jcb/article-pdf/181/6/1013/1551983/jcb_200711129.pdf by guest on 08 February 2026

cell polarization and directional migration through Src kinase and Rho GTPases. *J. Cell Biol.* 177:683–694.

Humphries, M.J., S.K. Akiyama, A. Komoriya, K. Olden, and K.M. Yamada. 1986. Identification of an alternatively spliced site in human plasma fibronectin that mediates cell type–specific adhesion. *J. Cell Biol.* 103:2637–2647.

Itoh, R.E., K. Kurokawa, Y. Ohba, H. Yoshizaki, N. Mochizuki, and M. Matsuda. 2002. Activation of rac and cdc42 video imaged by fluorescent resonance energy transfer-based single-molecule probes in the membrane of living cells. *Mol. Cell. Biol.* 22:6582–6591.

Kinnunen, T., M. Kaksonen, J. Saarinen, N. Kalkkinen, H.B. Peng, and H. Rauvala. 1998. Cortactin-Src kinase signaling pathway is involved in N-syndecan-dependent neurite outgrowth. *J. Biol. Chem.* 273:10702–10708.

Koo, B.K., Y.S. Jung, J. Shin, I. Han, E. Mortier, P. Zimmermann, J.R. Whiteford, J.R. Couchman, E.S. Oh, and W. Lee. 2006. Structural basis of syndecan-4 phosphorylation as a molecular switch to regulate signaling. *J. Mol. Biol.* 355:651–663.

Lim, S.T., R.L. Longley, J.R. Couchman, and A. Woods. 2003. Direct binding of syndecan-4 cytoplasmic domain to the catalytic domain of protein kinase C alpha (PKC alpha) increases focal adhesion localization of PKC alpha. *J. Biol. Chem.* 278:13795–13802.

Makarem, R., P. Newham, J.A. Askari, L.J. Green, J. Clements, M. Edwards, M.J. Humphries, and A.P. Mould. 1994. Competitive binding of vascular cell adhesion molecule-1 and the HepII/IIICS domain of fibronectin to the integrin alpha 4 beta 1. *J. Biol. Chem.* 269:4005–4011.

Mammoto, A., S. Huang, and D.E. Ingber. 2007. Filamin links cell shape and cytoskeletal structure to Rho regulation by controlling accumulation of p190RhoGAP in lipid rafts. *J. Cell Sci.* 120:456–467.

Morgan, M.R., M.J. Humphries, and M.D. Bass. 2007. Synergistic control of cell adhesion by integrins and syndecans. *Nat. Rev. Mol. Cell Biol.* 8:957–969.

Nimnual, A.S., L.J. Taylor, and D. Bar-Sagi. 2003. Redox-dependent downregulation of Rho by Rac. *Nat. Cell Biol.* 5:236–241.

Nobes, C.D., and A. Hall. 1995. Rho, rac, and cdc42 GTPases regulate the assembly of multimolecular focal complexes associated with actin stress fibers, lamellipodia, and filopodia. *Cell.* 81:53–62.

Noren, N.K., W.T. Arthur, and K. Burridge. 2003. Cadherin engagement inhibits RhoA via p190RhoGAP. *J. Biol. Chem.* 278:13615–13618.

Pertz, O., L. Hodgson, R.L. Klemke, and K.M. Hahn. 2006. Spatiotemporal dynamics of RhoA activity in migrating cells. *Nature.* 440:1069–1072.

Raftopoulou, M., and A. Hall. 2004. Cell migration: Rho GTPases lead the way. *Dev. Biol.* 265:23–32.

Ren, X.D., W.B. Kiosses, and M.A. Schwartz. 1999. Regulation of the small GTP-binding protein Rho by cell adhesion and the cytoskeleton. *EMBO J.* 18:578–585.

Roof, R.W., M.D. Haskell, B.D. Dukes, N. Sherman, M. Kinter, and S.J. Parsons. 1998. Phosphotyrosine (p-Tyr)-dependent and -independent mechanisms of p190 RhoGAP-p120 RasGAP interaction: Tyr 1105 of p190, a substrate for c-Src, is the sole p-Tyr mediator of complex formation. *Mol. Cell. Biol.* 18:7052–7063.

Sharma, A., J.A. Askari, M.J. Humphries, E.Y. Jones, and D.I. Stuart. 1999. Crystal structure of a heparin- and integrin-binding segment of human fibronectin. *EMBO J.* 18:1468–1479.

Takagi, J., H.P. Erickson, and T.A. Springer. 2001. C-terminal opening mimics 'inside-out' activation of integrin alpha5beta1. *Nat. Struct. Biol.* 8:412–416.

Tkachenko, E., A. Elfenbein, D. Tirziu, and M. Simons. 2006. Syndecan-4 clustering induces cell migration in a PDZ-dependent manner. *Circ. Res.* 98:1398–1404.

Wang, R., R.A. Clark, D.F. Mosher, and X.D. Ren. 2005. Fibronectin's central cell-binding domain supports focal adhesion formation and Rho signal transduction. *J. Biol. Chem.* 280:28803–28810.

Weinbaum, S., J.M. Tarbell, and E.R. Damiano. 2007. The structure and function of the endothelial glycocalyx layer. *Annu. Rev. Biomed. Eng.* 9:121–167.

Wilcox-Adelman, S.A., F. Denhez, and P.F. Goetinck. 2002. Syndecan-4 modulates focal adhesion kinase phosphorylation. *J. Biol. Chem.* 277:32970–32977.

Wildenberg, G.A., M.R. Dohn, R.H. Carnahan, M.A. Davis, N.A. Lobdell, J. Settleman, and A.B. Reynolds. 2006. p120-catenin and p190RhoGAP regulate cell-cell adhesion by coordinating antagonism between Rac and Rho. *Cell.* 127:1027–1039.

Woods, A., J.R. Couchman, S. Johansson, and M. Hook. 1986. Adhesion and cytoskeletal organisation of fibroblasts in response to fibronectin fragments. *EMBO J.* 5:665–670.

Woods, A., R.L. Longley, S. Tumova, and J.R. Couchman. 2000. Syndecan-4 binding to the high affinity heparin-binding domain of fibronectin drives focal adhesion formation in fibroblasts. *Arch. Biochem. Biophys.* 374:66–72.

Downloaded from http://rupress.org/jcb/article-pdf/181/6/1013/1551983/jcb_200711129.pdf by guest on 08 February 2026